

Steady-state localized-delocalized phase transition of an incoherent-pumped dissipative Bose-Hubbard model

Yuanwei Zhang,^{1,2} Jingtao Fan,^{3,4} Gang Chen,^{3,4,*} and Wu-Ming Liu^{1,2,†}

¹Beijing National Laboratory for Condensed Matter Physics,

Institute of Physics, Chinese Academy of Sciences, Beijing 100190, China

²School of Physical Sciences, University of Chinese Academy of Sciences, Beijing 100190, China

³State Key Laboratory of Quantum Optics and Quantum Optics Devices,

Institute of Laser Spectroscopy, Shanxi University, Taiyuan, Shanxi 030006, China

⁴Collaborative Innovation Center of Extreme Optics,
Shanxi University, Taiyuan, Shanxi 030006, China

We investigate steady-state properties of a two-dimensional incoherent-pumped dissipative Bose-Hubbard model, which describes a photon square lattice. This incoherent pumping exhibits an important environment-induced higher-order fluctuation effect, which induces a strong competition between the driven-dissipative channel, the photon-photon interaction, and the photon hopping in multi-photon processes. This new competition gives rise to a spontaneous breaking of the $U(1)$ symmetry of system. As a result, we predict a many-body steady-state localized-delocalized phase transition and an anti-blockade effect, in which the increasing of the repulsive photon-photon interaction promotes the emergence of phase transition. These unconventional many-body steady-state phenomena can be understood by analyzing the single-cavity properties. Our results pave a new way to control many-body dynamics of driven-dissipative systems.

PACS numbers: 03.65.Yz, 67.25.dj, 42.50.Pq

Introduction.—Understanding and controlling quantum many-particle systems is an fundamental task but a grand challenge in modern physics. A crucial problem is that almost all many-particle systems are coupled to the environment and thus are subjected to unavoidable dissipations, which are usually compensated by external incident laser fields. Recently, both theoretical [1–10] and experimental [11–13] works have demonstrated that the dissipations can create correlations between particles and represents the dominate resource of many-body dynamics. Following this pioneer discovery, driving-dissipative many-body systems have attracted great attention, and especially, new many-body correlation characters far from thermal equilibrium have been revealed [14–43].

In addition to the dissipation processes, the coupling with the environment also induces actual random fluctuating driven processes. In thermal equilibrium case, they are not independent but completely determine each other through the fluctuation–dissipation theorem. This mechanism is the origin of random phenomena, which are the key to understand the complexity of real word. In classical case, the most famous example is the Brownian motion of particles [44]. And in quantum scale, these effects have been proved to play an important role, for example, in determining the cooling limit of optomechanical systems [45]. In general, the random fluctuating force induces the thermal noise, which is harmful for studying quantum phase transitions and should be inhibited by reducing the temperature of the environment. In this Letter, we reveal that the fluctuating driven processes can generate exotic steady-state phases and phase tran-

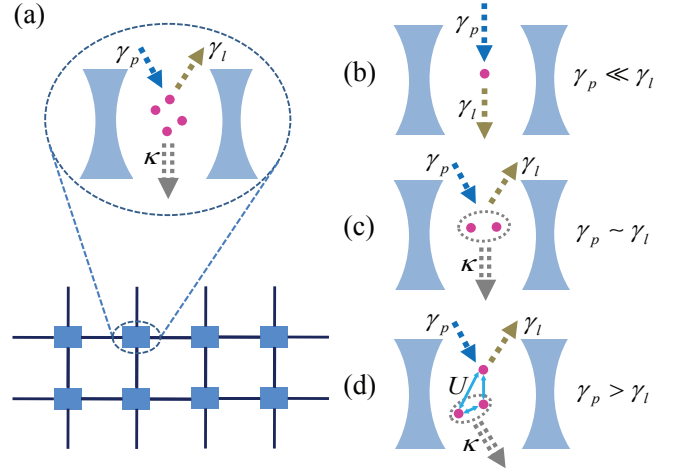


FIG. 1: (a) Sketch of a photon square lattice made of non-linear cavities, with the incoherent-pumped process γ_p , the single-photon loss process γ_l , and the two-photon loss process κ . (b)-(d) Schematics of the single-cavity driven-dissipative processes for different parameters, such that (b) $\gamma_p \ll \gamma_l$, (c) $\gamma_p \sim \gamma_l$, and (d) $\gamma_p > \gamma_l$.

sitions in non-equilibrium systems.

To show our arguments, we consider a two-dimensional (2D) incoherent-pumped dissipative Bose-Hubbard (BH) model [46–50], which describes a photon square lattice shown in Fig. 1(a) [51]. The incoherent-pumped process, realized in experiments [46–50, 52], is a kind of random driven process. Here, this incoherent pumping induces a strong competition between the driven-dissipative channel, the photon-photon interaction, and

the photon hopping in multi-photon processes. This new competition gives rise to a spontaneous breaking of the $U(1)$ symmetry of system. As a result, we predict a many-body steady-state localized-delocalized phase transition and an anti-blockade effect [53], in which the increasing of the repulsive photon-photon interaction promotes the emergence of phase transition. We emphasize that the steady-state phenomena predicted can be understood by analyzing the single-cavity properties, and have no correspondence in equilibrium case. Moreover, they are fully governed by the multi-photon processes, arising from the environment-induced higher-order fluctuations. However, in the mean-field level these multi-photon processes are usually neglected and the relevant physics cannot be captured. To overcome this shortcoming, we introduce a non-equilibrium Green's function approach.

Incoherent-pumped dissipative Bose-Hubbard model.—The incoherent-pumped dissipative dynamics of the 2D BH model is governed by the following Lindblad master equation of the many-body density matrix $\rho(t)$ ($\hbar = 1$ hereafter) [46]:

$$\begin{aligned} \partial_t \rho = & -i[H, \rho] + \gamma_p \sum_i \left(a_i^\dagger \rho a_i - \frac{1}{2} [a_i a_i^\dagger, \rho]_+ \right) \\ & + \gamma_l \sum_i \left(a_i \rho a_i^\dagger - \frac{1}{2} [a_i^\dagger a_i, \rho]_+ \right) \\ & + \kappa \sum_i \left(a_i a_i \rho a_i^\dagger a_i^\dagger - \frac{1}{2} [a_i^\dagger a_i^\dagger a_i a_i, \rho]_+ \right), \quad (1) \end{aligned}$$

with

$$H = -\frac{J}{z} \sum_{\langle i,j \rangle} a_i^\dagger a_j + \omega_c \sum_i a_i^\dagger a_i + \frac{U}{2} \sum_i a_i^\dagger a_i^\dagger a_i a_i. \quad (2)$$

In Eq. (1), $[\cdots]_+$ is the anticommutator, a_i^\dagger creates a photon on site i , γ_p describes the incoherent-pumped process, and γ_l and κ govern respectively the single- and two-photon loss processes [54]. In the BH Hamiltonian (2), $\langle i, j \rangle$ indicates that the photon can hop between adjacent cavities, $J > 0$ is the hopping strength, $z = 4$ is the coordination number, ω_c is the photon frequency, and $U > 0$ represents the repulsive photon-photon interaction [54].

Since the injected photons from the incoherent pumping obey random distribution, Eq. (1) still holds a global $U(1)$ symmetry. More interestingly, the environment-induced higher-order fluctuations induce multi-photon processes, in which the driven-dissipative channel has a strong competition with the photon-photon interaction and the photon hopping. This new competition gives rise to a spontaneous breaking of the $U(1)$ symmetry, and thus a many-body steady-state phase transition, from a localized state (LS) to a delocalized (superfluid) state (DS), is expected to emerge [55].

To better understand relevant physics, we begin to qualitatively analyze a single-cavity problem. When

$\gamma_p \ll \gamma_l$, the single-photon loss process makes the injected photons decay to the environment very fast; see Fig. 1(b). When $\gamma_p \sim \gamma_l$, the probability of photons staying in the cavity becomes larger and two photons maybe appear at the same time. Hence, the two-photon loss channel opens; see Fig. 1(c). When $\gamma_p > \gamma_l$, there exists an effective gain of photons through the single-particle process. In this case, multiple photons maybe appear in the cavity and the probability of the two-photon loss event is increased. As a result, the effective gain process is balanced by the two-photon loss process; see Fig. 1(d). Interestingly, in this region the photon-photon interaction plays a crucial role in determining the systematic properties. Especially, when it is strong, the photons oscillate faster and the relative possibility of the dissipative events is decreased. It implies that the photon-photon interaction not only governs the excitation energy of the multi-photon state, but also increases the linewidth of excitation [56]. If the linewidth is divergent, the steady state, with random distribution of multiple photons discussed above, becomes unstable, and thus a new steady state emerges, since the photon-photon interaction makes the photons tend to oscillate with a uniform phase.

For the photon square lattice, the many-body steady state is the result of the detailed balance between the photon input and output processes of each cavity. It refers to not only the driven-dissipative processes but also the photon hopping between adjacent cavity. When the hopping strength becomes strong enough, the photons can hop in all lattices without decay into the environment. Therefore, a steady-state phase transition, from the LS to the DS, occurs. However, in the mean-field level these multi-photon processes discussed above are usually neglected and the relevant many-body physics cannot be captured [57]. To overcome this shortcoming, here we introduce a non-equilibrium Green's function approach.

Noise state of the single cavity.—Similar to the previous qualitative analysis, we also begin to quantitatively consider a single-cavity case, in which a_i is replaced by a . We mainly capture its single-particle excitation spectra by calculating the retard Green's function $G_0^R(t) = -i\theta(t) \langle [a(t), a^\dagger(0)] \rangle$ [58], where $\theta(t)$ is the Heaviside step function. A simple way to obtain $G_0^R(t)$ is taken into account its dynamics, $i\dot{G}_0^R(t) = \delta(t) - \theta(t) \langle [(i\omega_c - \chi)a(t), a^\dagger(0)] \rangle - \theta(t) \langle [(iU + \kappa)a^\dagger a^2(t), a^\dagger(0)] \rangle$ [59], where $\delta(t)$ is the delta function and $\chi = (\gamma_p - \gamma_l)/2$ describes the effective gain of photons through the single-particle process.

The term $-i\theta(t) \langle [a^\dagger a^2(t), a^\dagger(0)] \rangle$ is called the second-order time-ordered correlation function, and can be obtained by the higher-order terms through general recursive relations [59]. It reflects the important environment-induced quantum fluctuation effect. Due to the existence of this term, the above dynamical equation is not a closed equation. In the mean-field level, this equation can be linearized and becomes a closed equa-

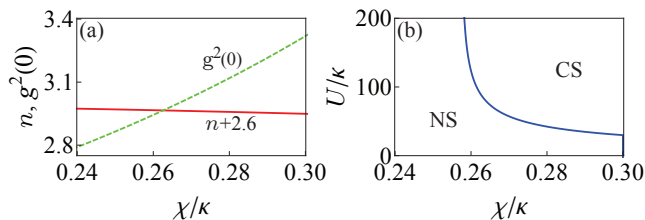


FIG. 2: (a) n and $g^2(0)$ in the noise state versus χ . (b) Steady-state phase diagram of the single cavity versus U and χ . Here, NS and CS denote the noise and coherent classical states, respectively. In these figures, $\gamma_p/\kappa = 0.60$ and the maximum of χ/κ is thus 0.30, according to the definition.

tion. Unfortunately, under this approximation the relevant physics will be lost [59]. In the following discussions, we carefully consider the higher-order time-ordered correlation functions.

In current experiments [60], the maximal photon number in the cavity is small. We assume that there are at most four incident photons, and then obtain the retard Green's function after neglecting the time-ordered correlation functions higher than the fourth order. We find that when U is weak, there exists a novel noise state, characterized by $\langle a \rangle = 0$ and $\langle a^\dagger a \rangle = n \neq 0$, which clearly demonstrates the random distribution of the photon field. It is quite different from the mean-field prediction [57], with a vacuum state ($\langle a \rangle = 0$ and $n = 0$). In Fig. 2(a), we plot the mean-photon number n and the second-order correlation function $g^2(0) = \langle a^{\dagger 2} a^2 \rangle / \langle a^\dagger a \rangle^2$ to show the features of the photon field distribution in the noise state. When increasing U , a steady-state phase transition, from a noise state to a coherent classical state ($\langle a \rangle \neq 0$ and $n \neq 0$), can be predicted [59]. In Fig. 2(b), we plot the corresponding phase diagram versus U and χ [61].

As shown in Fig. 2(a), when increasing χ , n is not increased, which means that the effective input photons are dissipated to the environment through the two-photon loss process. On the contrary, $g^2(0)$ is increased, which implies that the environment-induced quantum fluctuations are enhanced, i.e., the probability of the multi-photon events becomes larger. As we discussed in qualitative analysis, the repulsive interaction between multiple photons will make the noise state become unstable. Therefore, the phase transition only occurs for a strong χ , as shown in Fig. 2(b), and moreover, the critical photon-photon interaction strength U_c is decreased when increasing χ . In contrast, when $\chi < 0.26$, U_c is rapidly increased to infinity and thus the phase transition could not happen. To gain deeper insight of phase transition, in Fig. 3 we plot the single-particle excitation spectra ω_0 , determined by the poles of the retarded Green's function in the frequency space. The real parts of ω_0 , abbreviated as $\text{Re}(\omega_0)$, reflect the excitation energies,

and the imaginary parts of ω_0 , abbreviated as $\text{Im}(\omega_0)$, govern the linewidths of the excitation spectra. When U is large enough, the excitation energies are given approximately by 0, U , $2U$, and $3U$, which correspond to the change of the total photon-photon interaction energy when adding or removing one photon. We also note that when increasing U , one branch of $\text{Im}(\omega_0)$ (the red line in Fig. 3), which corresponds to excitation of the multi-photon state, is increased. If χ is small ($\chi = 0.20$), it becomes a negative constant. On the contrary, when χ is large ($\chi = 0.27$), it will reach 0 for a strong U . This means the lifetime of excitation is divergent, and thus the noise state becomes instable.

It should be emphasized that the noise state and the properties of the excitation spectra of the single cavity are crucial for exploring and understanding the many-body steady-state phase transition for the 2D incoherent-pumped dissipative BH model, governed by the Lindblad master equation (1).

Many-body steady-state phase transition.—To explore the many-body steady-state properties of Eq. (1), we first assume that every cavity is initially prepared in its noise state, which means that the photons are localized at each site. Then, we introduce the Keldysh functional-integral formalism to calculate the full retard Green's function $\tilde{G}^R(t) = -i \langle a_{i,cl}(t) a_{i,q}^*(0) \rangle$ [62], which is dressed by the hopping terms. In details, we use a non-equilibrium linked-cluster expansion approach, which gives a description of equilibrium or non-equilibrium strong correlation systems within the same formalism [62–64]. Following this method, all the single-site terms are regarded as the unperturbed parts and the hopping terms are treated as perturbations [65].

We sum an infinite set of diagrams by calculating the irreducible part of the retard Green's function

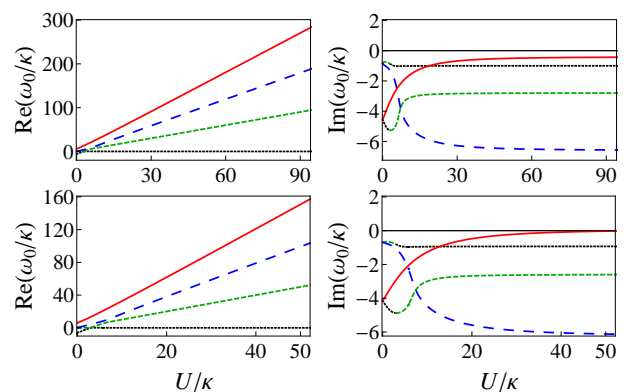


FIG. 3: The single-particle excitation spectra of the single cavity versus U for $\chi/\kappa = 0.20$ (upper panel) and $\chi/\kappa = 0.27$ (lower panel), with $\gamma_p/\kappa = 0.60$. Since there are at most four incident photons in the cavity, the excitation spectra have four branches, which are labeled by different linetypes and colors.

$K^R(t)$, which is connected, in the frequency space, to the full Green's function via the following equation: $\tilde{G}^R(\mathbf{k}, \omega) = K^R(\mathbf{k}, \omega) / [1 - J(\mathbf{k}) K^R(\mathbf{k}, \omega)]$, with the 2D lattice dispersion $J(\mathbf{k}) = 2J \cos(\mathbf{k} \cdot \mathbf{r})$, where \mathbf{k} is the wave vector and \mathbf{r} is the lattice vector, with $|\mathbf{r}| = 1$. We mainly consider the contribution of the chain diagram to $K^R(t)$. By setting $K^R(\omega) = G_0^R(\omega)$, where $G_0^R(\omega)$ is the single-cavity retard Green's function in the frequency-momentum space, we can obtain a non-equilibrium Dyson equation about the inverse of the full retard Green's function, i.e.,

$$[\tilde{G}^R(\mathbf{k}, \omega)]^{-1} = [G_0^R(\omega)]^{-1} - \Sigma^R(\mathbf{k}, \omega), \quad (3)$$

where $\Sigma^R(\mathbf{k}, \omega) = J(\mathbf{k})$ is the self-energy [65].

Equation (3) is the main result of this Letter. Although this equation is similar to that in equilibrium case, the undertaken physics is quite different, because it contains all the driven-dissipative terms. For equilibrium case, a many-body phase transition, whose phase boundary is characterized by the free energy, emerges. Whereas for non-equilibrium case considered here, we donot have a sensible notion of a free energy and a many-body steady-state phase transition is expected to occur. Moreover, the corresponding phase boundary is completely determined by the characteristic frequencies $\tilde{\omega}$ of the single-particle excitation spectra, which are the poles of $\tilde{G}^R(\mathbf{k}, \omega)$, i.e., $[\tilde{G}^R(\mathbf{k}, \tilde{\omega})]^{-1} = 0$. When the imaginary parts of $\tilde{\omega}$ are negative, a localized steady state is stable, otherwise this state is unstable and a delocalized steady state emerges.

In Fig. 4(a), we plot the many-body steady-state phase diagram versus U and J , with the same driven-dissipative parameters as the upper panel of Fig. 3. For a weak U , the driven-dissipative induced dephasing is dominant and no steady-state phase transition can be found, as expected. When U is strong, it suppresses the dephasing effect and all linewidths of the single-cavity excitations become constant; see Fig. 3. Thus, the many-body steady-state LS-DS phase transition occurs, and more-

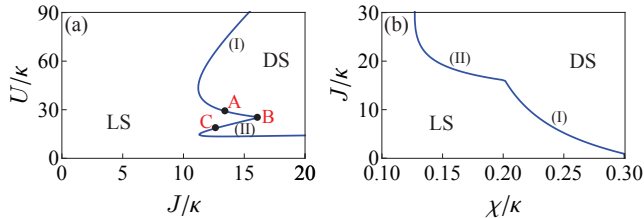


FIG. 4: (a) Many-body steady-state phase diagram versus J and U for $\chi/\kappa = 0.2$ and $\gamma_p/\kappa = 0.6$. A, B, and C are the chosen points, whose different excitation spectra are presented in Fig. 5. (b) Phase diagram versus J and χ for $U/\kappa = 25$ and $\gamma_p/\kappa = 0.6$. In these figures, (I) and (II) label the different kinds of the phase transition, from the localized state (LS) and delocalized state (DS).

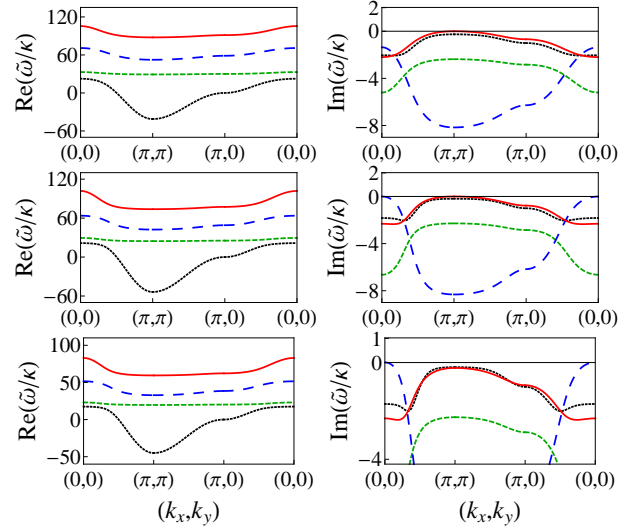


FIG. 5: Energy-momentum dispersions of elementary excitations for points A (upper panel), B (middle panel), and C (lower panel), indicated in Fig. 4(a). $(0, 0)$, (π, π) , and $(\pi, 0)$ are the special points in the Brillouin zone of the square lattice. Here, the elementary excitations have four branches, which are labeled by different linetypes and colors.

over, is dominated by the competition between U and J . These predicted results are sharply contrast to those derived from the mean-field level [66], in which the important environment-induced quantum fluctuations have been neglected.

More interestingly, for an intermediate U , the single-cavity excitations are very complex, and the many-body steady-state phase diagram exhibits unconventional behaviors. For example, the phase boundary is consisted of two smooth curves, which are labeled respectively as (I) and (II) and connected together at a tip (point B). We emphasize that these two curves reflect different features of phase transition. In curve (I), the instabilities arise at $k = (\pi, \pi)$, corresponding to a multi-photon model (red line), while in curve (II), the instabilities arise at $k = (0, 0)$, corresponding to a photon-pair model (blue line). At the tip, the instabilities arise from $k = (\pi, \pi)$ and $k = (0, 0)$ at the same time. These properties can be confirmed in Fig. 5, in which we plot the energy-momentum dispersions of the elementary excitations for points A, B, and C, indicated in Fig. 4(a). These properties can be explained as follows. When increasing the relatively small U , the linewidth of excitation, which corresponds to the photon-pair model, is dramatically decreased (see the blue line in Fig. 3). This means that the photon-photon interaction makes two photons tend to be oscillating with same phases, which enhances the two-photon loss process. In this case, when increasing J , the photons will hop into adjacent cavities if they have same phases. As a result, this phase consistency promotes the

emergence of the many-body steady-state phase transition, with $k = (0, 0)$. When U is large, the maximal $\text{Im}(\omega_0)$ corresponds to the excitation of the multi-photon state (see the red line in Fig. 3). In this case, the photons are more likely tunneling into adjacent cavities if they have opposite phases to overcome the repulsive interaction. Thus, the instabilities arise from $k = (\pi, \pi)$. A similar phenomenon can be found in Fig. 4(b), in which when increasing χ , the multi-photon processes play a dominate role and the most instable mode changes from $k = (0, 0)$ to $k = (\pi, \pi)$.

In addition, when increasing U for a fixed $J/\kappa (= 15)$, we observe two LS-DS-LS phase transitions; see also Fig. 4(a). The first one shows that the DS only occurs when U is large enough as we discussed above. When increasing U , the system goes back into the LS. This property is attributed to the competition between U and J and reflects a photon blockade effect. When further increasing U , the second LS-DS-LS phase transition occurs. This means that there exists a anti-blockade effect, in which the increasing of U promotes the emergence of phase transition. The main reason is that when increasing U , the linewidth of the excitation of the multi-photon state becomes longer (see the red line in Fig. 3) and the photons are more easily to enter the adjacent cavities.

Conclusions.—In summary, we have explored the non-equilibrium physics of a 2D incoherent-pumped dissipative BH model, by introducing a non-equilibrium Green's function approach. We have predicted a many-body steady-state localized-delocalized phase transition and revealed an interesting anti-blockade effect. We have shown that all unconventional many-body steady-state features arise from the environment-induced higher-order fluctuations and can be explained by analyzing the single-cavity properties. Our results pave a new way to control many-body dynamics of driven-dissipative systems.

We thank Prof. Rosario Fazio, Prof. Hendrik Weimer, and Dr. Yu Chen for numerous insightful discussions. This work was supported in part by the NKRD under Grants No. 2012CB821305 and No. 2016YFA0301500; the NSFC under Grants No. 61227902, No. 61275211, No. 61378017, No. 11422433, No. 11434015, and No. 11674200; SKLQOQOD under Grants No. KF201403; SPRPCAS under Grants No. XDB01020300 and No. XDB21030300; the FANEDD under Grant No. 201316; OYTPSP; and SSCC.

* chengang971@163.com

† wmlu@iphy.ac.cn

- [1] S. Diehl, A. Micheli, A. Kantian, B. Kraus, H. P. Büchler, and P. Zoller, Quantum states and phases in driven open quantum systems with cold atoms, *Nat. Phys.* **4**, 878 (2008).

- [2] F. Verstraete, M. M. Wolf, and J. I. Cirac, Quantum computation and quantum-state engineering driven by dissipation, *Nat. Phys.* **5**, 633 (2009).
- [3] H. Weimer, M. Müller, I. Lesanovsky, P. Zoller, and H. P. Büchler, A Rydberg quantum simulator, *Nat. Phys.* **6**, 382 (2010).
- [4] S. Diehl, W. Yi, A. J. Daley, and P. Zoller, Dissipation-Induced d-Wave Pairing of Fermionic Atoms in an Optical Lattice, *Phys. Rev. Lett.* **105**, 227001 (2010).
- [5] D. D. B. Rao and K. Mølmer, Dark Entangled Steady States of Interacting Rydberg Atoms, *Phys. Rev. Lett.* **111**, 033606 (2013).
- [6] A. W. Carr and M. Saffman, Preparation of Entangled and Antiferromagnetic States by Dissipative Rydberg Pumping, *Phys. Rev. Lett.* **111**, 033607 (2013).
- [7] B. Bellomo and M. Antezza, Nonequilibrium dissipation-driven steady many-body entanglement, *Phys. Rev. A* **91**, 042124 (2015).
- [8] M. Abdi, P. Degenfeld-Schonburg, M. Sameti, C. Navarrete-Benlloch, and M. J. Hartmann, Dissipative Optomechanical Preparation of Macroscopic Quantum Superposition States, *Phys. Rev. Lett.* **116**, 233604 (2016).
- [9] M. Žnidarič, Dissipative Remote-State Preparation in an Interacting Medium, *Phys. Rev. Lett.* **116**, 030403 (2016).
- [10] F. Reiter, D. Reeb, and A. S. Sørensen, Scalable dissipative preparation of many-body entanglement, *Phys. Rev. Lett.* **117**, 040501 (2016).
- [11] H. Krauter, C. A. Muschik, K. Jensen, W. Wasilewski, J. M. Petersen, J. I. Cirac, and E. S. Polzik, Entanglement Generated by Dissipation and Steady State Entanglement of Two Macroscopic Objects, *Phys. Rev. Lett.* **107**, 080503 (2011).
- [12] J. T. Barreiro, M. Müller, P. Schindler, D. Nigg, T. Monz, M. Chwalla, M. Hennrich, C. F. Roos, P. Zoller, and R. Blatt, An open-system quantum simulator with trapped ions, *Nature (London)* **470**, 486 (2011).
- [13] P. Schindler, M. Müller, D. Nigg, J. T. Barreiro, E. A. Martinez, M. Hennrich, T. Monz, S. Diehl, P. Zoller, and R. Blatt, Quantum simulation of dynamical maps with trapped ions, *Nat. Phys.* **9**, 361 (2013).
- [14] S. Diehl, A. Tomadin, A. Micheli, R. Fazio, and P. Zoller, Dynamical Phase Transitions and Instabilities in Open Atomic Many-Body Systems, *Phys. Rev. Lett.* **105**, 015702 (2010).
- [15] S. Diehl, E. Rico, M. A. Baranov, and P. Zoller, Topology by dissipation in atomic quantum wires, *Nat. Phys.* **7**, 971 (2011).
- [16] A. Tomadin, S. Diehl, and P. Zoller, Nonequilibrium phase diagram of a driven and dissipative many-body system, *Phys. Rev. A* **83**, 013611 (2011).
- [17] F. Nissen, S. Schmidt, M. Biondi, G. Blatter, H. E. Türeci, and J. Keeling, Nonequilibrium Dynamics of Coupled Qubit-Cavity Arrays, *Phys. Rev. Lett.* **108**, 233603 (2012).
- [18] C.-E. Bardyn, M. A. Baranov, E. Rico, A. Imamoglu, P. Zoller, and S. Diehl, Majorana Modes in Driven-Dissipative Atomic Superfluids with a Zero Chern Number, *Phys. Rev. Lett.* **109**, 130402 (2012).
- [19] L. M. Sieberer, S. D. Huber, E. Altman, and S. Diehl, Dynamical Critical Phenomena in Driven-Dissipative Systems, *Phys. Rev. Lett.* **110**, 195301 (2013); Nonequilibrium functional renormalization for driven-dissipative

- Bose-Einstein condensation, Phys. Rev. B **89**, 134310 (2014).
- [20] A. Le Boité, G. Orso, and C. Ciuti, Steady-State Phases and Tunneling-Induced Instabilities in the Driven Dissipative Bose-Hubbard Model, Phys. Rev. Lett. **110**, 233601 (2013); Bose-Hubbard model: Relation between driven-dissipative steady states and equilibrium quantum phases, Phys. Rev. A **90**, 063821 (2014).
- [21] M. Marcuzzi, E. Levi, S. Diehl, J. P. Garrahan, and I. Lesanovsky, Universal Nonequilibrium Properties of Dissipative Rydberg Gases, Phys. Rev. Lett. **113**, 210401 (2014).
- [22] J. Jin, D. Rossini, M. Leib, M. J. Hartmann, and R. Fazio, Steady-state phase diagram of a driven QED-cavity array with cross-Kerr nonlinearities, Phys. Rev. A **90**, 023827 (2014).
- [23] L. Bonnes, D. Charrier, and A. M. Läuchli, Dynamical and steady-state properties of a Bose-Hubbard chain with bond dissipation: A study based on matrix product operators, Phys. Rev. A **90**, 033612 (2014).
- [24] H. Weimer, Variational Principle for Steady States of Dissipative Quantum Many-Body Systems, Phys. Rev. Lett. **114**, 040402 (2015); Variational analysis of driven-dissipative Rydberg gases, Phys. Rev. A **91**, 063401 (2015).
- [25] J. Cui, J. I. Cirac, and M. C. Bañuls, Variational Matrix Product Operators for the Steady State of Dissipative Quantum Systems, Phys. Rev. Lett. **114**, 220601 (2015).
- [26] D. Nagy and P. Domokos, Nonequilibrium Quantum Criticality and Non-Markovian Environment: Critical Exponent of a Quantum Phase Transition, Phys. Rev. Lett. **115**, 043601 (2015).
- [27] S. Finazzi, A. Le Boité, F. Storme, A. Baksic, and C. Ciuti, Corner-space renormalization method for driven-dissipative two-dimensional correlated systems, Phys. Rev. Lett. **115**, 080604 (2015).
- [28] G. Dagvadorj, J. M. Fellows, S. Matyjaśkiewicz, F. M. Marchetti, I. Carusotto, and M. H. Szymańska, Nonequilibrium Phase Transition in a Two-Dimensional Driven Open Quantum System, Phys. Rev. X **5**, 041028 (2015).
- [29] J. C. Budich, P. Zoller, and S. Diehl, Dissipative preparation of Chern insulators, Phys. Rev. A **91**, 042117 (2015).
- [30] C.-K. Chan, T. E. Lee, and S. Gopalakrishnan, Limit-cycle phase in driven-dissipative spin systems, Phys. Rev. A **91**, 051601 (2015).
- [31] N. Lang and H. P. Büchler, Exploring quantum phases by driven dissipation, Phys. Rev. A **92**, 012128 (2015).
- [32] E. Mascarenhas, H. Flayac, and V. Savona, Matrix-product-operator approach to the nonequilibrium steady state of driven-dissipative quantum arrays, Phys. Rev. A **92**, 022116 (2015).
- [33] L. M. Sieberer, M. Buchhold, and S. Diehl, Keldysh Field Theory for Driven Open Quantum Systems, arXiv: 1512.00637 (2015).
- [34] J. Marino and S. Diehl, Driven Markovian Quantum Criticality, Phys. Rev. Lett. **116**, 070407 (2016).
- [35] M. Schiró C. Joshi, M. Bordyuh, R. Fazio, J. Keeling, and H. E. Türeci, Exotic Attractors of the Nonequilibrium Rabi-Hubbard Model, Phys. Rev. Lett. **116**, 143603 (2016).
- [36] R. Labouvie, B. Santra, S. Heun, and H. Ott, Bistability in a Driven-Dissipative Superfluid, Phys. Rev. Lett. **116**, 235302 (2016).
- [37] A. H. Werner, D. Jaschke, P. Silvi, M. Kliesch, T. Calarco, J. Eisert, and S. Montangero, Positive Tensor Network Approach for Simulating Open Quantum Many-Body Systems, Phys. Rev. Lett. **116**, 237201 (2016).
- [38] E. Levi, M. Heyl, I. Lesanovsky, and J. P. Garrahan, Robustness of Many-Body Localization in the Presence of Dissipation, Phys. Rev. Lett. **116**, 237203 (2016).
- [39] A. C. Y. Li, F. Petruccione, and J. Koch, Resummation for Nonequilibrium Perturbation Theory and Application to Open Quantum Lattices, Phys. Rev. X **6**, 021037 (2016).
- [40] J. Jin, A. Biella, O. Viyuela, L. Mazza, J. Keeling, R. Fazio, and D. Rossini, Cluster Mean-Field Approach to the Steady-State Phase Diagram of Dissipative Spin Systems, Phys. Rev. X **6**, 031011 (2016).
- [41] B. Everest, M. Marcuzzi, and I. Lesanovsky, Atomic loss and gain as a resource for nonequilibrium phase transitions in optical lattices, Phys. Rev. A **93**, 023409 (2016).
- [42] J. J. Mendoza-Arenas, S. R. Clark, S. Felicetti, G. Romero, E. Solano, D. G. Angelakis, and D. Jaksch, Beyond mean-field bistability in driven-dissipative lattices: Bunching-antibunching transition and quantum simulation, Phys. Rev. A **93**, 023821 (2016).
- [43] M. F. Maghrebi and A. V. Gorshkov, Nonequilibrium many-body steady states via Keldysh formalism, Phys. Rev. B **93**, 014307 (2016).
- [44] R. P. Feynman, *The Feynman Lectures on Physics* (Addison-Wesley, Reading, MA, 1965), Vol. I.
- [45] See, for example, a review, M. Aspelmeyer, T. J. Kippenberg, and F. Marquardt, Cavity optomechanics, Rev. Mod. Phys. **86**, 1391 (2014).
- [46] I. Carusotto and C. Ciuti, Quantum Fluids of Light, Rev. Mod. Phys. **85**, 299 (2013).
- [47] J. Kasprzak, M. Richard, S. Kundermann, A. Baas, P. Jeambrun, J. M. J. Keeling, F. M. Marchetti, M. H. Szymańska, R. André, J. L. Staehli, V. Savona, P. B. Littlewood, B. Deveaud, and Le Si Dang, Bose-Einstein condensation of exciton polaritons, Nature (London) **443**, 409, (2006).
- [48] D. Bajoni, E. Semenova, A. Lemaître, S. Bouchoule, E. Wertz, P. Senellart, and J. Bloch, Polariton light-emitting diode in a GaAs-based microcavity, Phys. Rev. B **77**, 113303 (2008).
- [49] S. I. Tsintzos, P. G. Savvidis, G. Deligeorgis, Z. Hatzopoulos, and N. T. Pelekanos, Room temperature GaAs exciton-polariton light emitting diode, Appl. Phys. Lett. **94**, 071109 (2009).
- [50] J. Keeling, F. M. Marchetti, M. H. Szymańska, and P. B. Littlewood, Collective coherence in planar semiconductor microcavities, Semicond. Sci. Technol. **22**, R1 (2007).
- [51] M. J. Hartmann, F. G. S. L. Brandã, and M. B. Plenio, Quantum many-body phenomena in coupled cavity arrays, Laser Photon. Rev. **2**, 527 (2008).
- [52] A. A. Houck, D. I. Schuster, J. M. Gambetta, J. A. Schreier, B. R. Johnson, J. M. Chow, L. Frunzio, J. Majer, M. H. Devoret, S. M. Girvin, and R. J. Schoelkopf, Generating single microwave photons in a circuit, Nature (London) **449**, 328 (2007).
- [53] In general, the strong interaction between the photons causes a photon blockade of cavity transmission, i.e., the presence of photons in the cavity can block the resonant injection of another photon [46].
- [54] A possible way to realize the photon-photon interaction is used the electromagnetically-induced transparency configuration [46]. In this case, the two-photon loss process

- can also appear naturally and be tuned independently.
- [55] For the equilibrium BH model, a $U(1)$ symmetry can be found. When this $U(1)$ symmetry is spontaneously broken, a phase transition, from a localized state to a delocalized (superfluid) state, emerges. See, for example, S. Sachdev, *Quantum Phase Transitions* (Cambridge University Press, Cambridge, England, 1999).
 - [56] In equilibrium case, the photon-photon interaction determines the photon distribution by minimizing the free energy. However, in nonequilibrium case we do not have a sensible notion of free energy, and the energy spectrum is defined in complex plane. Its real and imaginary parts reflect the excitation energy and linewidth, respectively.
 - [57] In Secs. (B) and (C) of Supplementary Material, we present the mean-field results of the single-cavity and many-body cases, respectively. In Sec. (D) of Supplementary Material, we use a continuous-field approximation in the Keldysh functional-integral formalism to study the many-body steady-state phase transition. We find that both these two methods cannot capture the expected many-body steady-state phase transition, because they neglect the important multi-photon processes, arising from the environment-induced higher-order fluctuations.
 - [58] In general, the retard Green's function is defined as $G_0^R(t, t') = -i\theta(t - t') \langle [a(t), a^\dagger(t')] \rangle$. Since we are interested in the steady-state properties, we assume that at time t' the system becomes steady, and then rewrite the retard Green's function as $G_0^R(t) = -i\theta(t) \langle [a(t), a^\dagger(0)] \rangle$.
 - [59] See Sec. (A) of Supplementary Material for more details.
 - [60] In current experiments of Rydberg atoms about the multi-photon electromagnetically-induced transparency [46], the maximal photon number in the cavity is small and tunable.
 - [61] Since the term $\omega_c a^\dagger a$ in the single-cavity Hamiltonian is eliminated by a unitary operator $R = \exp(i\omega_c t)$, the phase diagram is independent of the photon frequency.
 - [62] A. Altland and B. Simons, *Condensed Matter Field Theory* (Cambridge University Press, 2010).
 - [63] T. D. Graß, F. E. A. dos Santos, and A. Pelster, Excitation spectra of bosons in optical lattices from the Schwinger-Keldysh calculation, *Phys. Rev. A* **84**, 013613 (2011).
 - [64] M. P. Kennett and D. Dalidovich, Schwinger-Keldysh approach to out-of-equilibrium dynamics of the Bose-Hubbard model with time-varying hopping, *Phys. Rev. A* **84**, 033620 (2011).
 - [65] See Sec. (E) of Supplementary Material for more details.
 - [66] Using the mean-field approximation or continuous-field approximation in the Keldysh functional-integral formalism, only the steady-state phase transition, from the incoherent vacuum state to the coherent classical state, can be found at the critical point $\chi_c = 0$. Moreover, the photon-photon interaction and photon hopping have no effect on this phase transition. See Secs. (C) and (D) of Supplementary Material for more details [57].

Supplementary Material “Steady-state localized-delocalized phase transition of an incoherent-pumped dissipative Bose-Hubbard model”

Yuanwei Zhang,^{1,2} Jingtao Fan,^{3,4} Gang Chen,^{3,4,*} and Wu-Ming Liu^{1,2,†}

¹*Beijing National Laboratory for Condensed Matter Physics,*

Institute of Physics, Chinese Academy of Sciences, Beijing 100190, China

²*School of Physical Sciences, University of Chinese Academy of Sciences, Beijing 100190, China*

³*State Key Laboratory of Quantum Optics and Quantum Optics Devices,*

Institute of Laser Spectroscopy, Shanxi University, Taiyuan, Shanxi 030006, China

⁴*Collaborative Innovation Center of Extreme Optics,*

Shanxi University, Taiyuan, Shanxi 030006, China

The notation used in this Supplemental Material follows that introduced in the main text.

A. NOISE STATE FOR FOUR PHOTON CASE

In this section, we predict a novel noise state by approximately solving the following dynamical equation of the single-cavity retard Green's function:

$$i\dot{G}_0^R(t) = \delta(t) - \theta(t) \langle [(i\omega_c - \chi) a(t), a^\dagger(0)] \rangle - \theta(t) \langle [(iU + \kappa) a^\dagger a^2(t), a^\dagger(0)] \rangle. \quad (\text{S1})$$

By defining

$$\langle \langle F(a(t), a^\dagger(t)); a^\dagger(0) \rangle \rangle = -i\theta(t) \langle [F(a(t), a^\dagger(t)), a^\dagger(0)] \rangle, \quad (\text{S2})$$

where $F(a(t), a^\dagger(t))$ is an arbitrary function of $a(t)$ and $a^\dagger(t)$, we obtain a recursive relation about the high-order time-ordered correlation functions in the real-time space as

$$i\frac{d}{dt} \langle \langle a^{\dagger l} a^m(t); a^\dagger(0) \rangle \rangle = \delta(t) \langle [a^{\dagger l} a^m(t), a^\dagger(0)] \rangle + \theta(t) \left\langle \left[\frac{d}{dt} a^{\dagger l} a^m(t), a^\dagger(0) \right] \right\rangle, \quad (\text{S3})$$

where l and m are integers. According to the quantum regression theorem [1], the second term on the right hand of Eq. (S3) depends on

$$\frac{d \langle a^{\dagger l} a^m(t) \rangle}{dt} = A_{lm} \langle a^{\dagger l} a^m(t) \rangle + B_{lm} \langle a^{\dagger l+1} a^{m+1}(t) \rangle + C_{lm} \langle a^{\dagger l-1} a^{m-1}(t) \rangle, \quad (\text{S4})$$

where

$$A_{lm} = i\omega_c(l-m) + i\frac{U}{2}[l(l-1) - m(m-1)] + \chi(l+m) - \frac{\kappa}{2}[l(l-1) + m(m-1)], \quad (\text{S5})$$

*chengang971@163.com

†wmlu@iphy.ac.cn

$$B_{lm} = iU(l - m) - \kappa(l + m), \quad (S6)$$

$$C_{lm} = \gamma_p l m. \quad (S7)$$

Equations (S3) and (S4) are our main results of the incoherent-pumped dissipative single cavity. Solving them, we can capture all information about the photon field distribution and the single-particle excitation spectra. In general, we cannot obtain the full solutions of Eqs. (S3) and (S4), since they depend crucially on the photon number. In current experiments [2], the maximal photon number in the cavity is small. In the following discussions, we assume that there are at most four incident photons, and then obtain Eqs. (S3) and (S4) after neglecting the time-ordered correlation functions higher than the fourth order.

We first qualitatively analyze the characteristics of Eq. (S4), which determines the photon field distribution. By setting $d\langle a^{\dagger l} a^m(t) \rangle / dt = 0$, we can capture the information about all kinds of the one-time correlation functions of steady state. In these correlation functions, the non-diagonal terms ($l \neq m$) reflect the coupling between different photon Fock states [1] and can be used as the criterion of coherence between photons. To understand that, we choose $l = 0$ and $m = 1$, which leads to a steady equation of $\langle a \rangle$, i.e., $(-i\omega_c + \chi) \langle a \rangle = (iU + \kappa) \langle a^{\dagger} a^2 \rangle$. This equation has a normal solution, with $\langle a \rangle = \langle a^{\dagger} a^2 \rangle = 0$, which describes an incoherent steady-state property of system. In addition, the diagonal terms ($l = m$) determine the mean-photon number $\langle a^{\dagger} a \rangle$ and its fluctuations [1]. When $l = m = 1$, we obtain a steady equation of $\langle a^{\dagger} a \rangle$ as $2\chi \langle a^{\dagger} a \rangle = 2\kappa \langle a^{\dagger 2} a^2 \rangle - \gamma_p$, which contains a constant γ_p , originating from the different time orders of a and a^{\dagger} in the single-photon pumping and loss processes. This constant reflects the environment-induced quantum fluctuations of driven-dissipative process and makes $\langle a^{\dagger} a \rangle \neq 0$ for any case. It should be emphasized that the above properties still remain in the higher-order non-diagonal and diagonal terms. Therefore, we find that the incoherent state, characterized by $\langle a \rangle = 0$ and $\langle a^{\dagger} a \rangle \neq 0$, is a *noise* state, rather than a vacuum state, with $\langle a \rangle = 0$ and $\langle a^{\dagger} a \rangle = 0$, which can be derived from the mean-field approximation (see the following section). The denomination of “noise” implies the dephasing of the photon field, with random phase and amplitude.

For four incident photons considered here, we can truncate Eqs. (S3) and (S4) to the fourth order. In such case, the complete expressions of the truncated Eqs. (S3) and (S4) in the frequency space are given by

$$\left\{ \begin{array}{l} \omega \langle \langle a; a^{\dagger} \rangle \rangle_{\omega} = 1 + (\omega_c + i\chi) \langle \langle a; a^{\dagger} \rangle \rangle_{\omega} + (U - i\kappa) \langle \langle a^{\dagger} a^2; a^{\dagger} \rangle \rangle_{\omega} \\ \omega \langle \langle a^{\dagger} a^2; a^{\dagger} \rangle \rangle_{\omega} = 2 \langle a^{\dagger} a \rangle + (\omega_c + U + 3i\chi - i\kappa) \langle \langle a^{\dagger} a^2; a^{\dagger} \rangle \rangle_{\omega} \\ \quad + 2i\gamma_p \langle \langle a; a^{\dagger} \rangle \rangle_{\omega} + (U - 3i\kappa) \langle \langle a^{\dagger 2} a^3; a^{\dagger} \rangle \rangle_{\omega} \\ \omega \langle \langle a^{\dagger 2} a^3; a^{\dagger} \rangle \rangle_{\omega} = 3 \langle a^{\dagger 2} a^2 \rangle + (\omega_c + 2U + 5i\chi - 4i\kappa) \langle \langle a^{\dagger 2} a^3; a^{\dagger} \rangle \rangle_{\omega} \\ \quad + 6i\gamma_p \langle \langle a^{\dagger} a^2; a^{\dagger} \rangle \rangle_{\omega} + (U - 5i\kappa) \langle \langle a^{\dagger 3} a^4; a^{\dagger} \rangle \rangle_{\omega} \\ \omega \langle \langle a^{\dagger 3} a^4; a^{\dagger} \rangle \rangle_{\omega} = 4 \langle a^{\dagger 3} a^3 \rangle + (\omega_c + 3U + 7i\chi - 9i\kappa) \langle \langle a^{\dagger 3} a^4; a^{\dagger} \rangle \rangle_{\omega} \\ \quad + 12i\gamma_p \langle \langle a^{\dagger 2} a^3; a^{\dagger} \rangle \rangle_{\omega} \end{array} \right. \quad (S8)$$

$$\left\{ \begin{array}{l} \frac{d\langle a \rangle}{dt} = (-i\omega_c + \chi) \langle a \rangle - (iU + \kappa) \langle a^\dagger a^2 \rangle \\ \frac{d\langle a^\dagger \rangle}{dt} = (i\omega_c + \chi) \langle a^\dagger \rangle - (-iU + \kappa) \langle a^{\dagger 2} a \rangle \\ \frac{d\langle a^\dagger a \rangle}{dt} = 2\chi \langle a^\dagger a \rangle - 2\kappa \langle a^{\dagger 2} a^2 \rangle + \gamma_p \\ \frac{d\langle a^{\dagger 2} a^2 \rangle}{dt} = (-i\omega_c - iU + 3\chi - \kappa) \langle a^\dagger a^2 \rangle - (iU + 3\kappa) \langle a^{\dagger 2} a^3 \rangle + 2\gamma_p \langle a \rangle \\ \frac{d\langle a^{\dagger 2} a \rangle}{dt} = (i\omega_c + iU + 3\chi - \kappa) \langle a^{\dagger 2} a \rangle - (-iU + 3\kappa) \langle a^{\dagger 3} a^2 \rangle + 2\gamma_p \langle a^\dagger \rangle \\ \frac{d\langle a^{\dagger 2} a^2 \rangle}{dt} = (4\chi - 2\kappa) \langle a^{\dagger 2} a^2 \rangle - 4\kappa \langle a^{\dagger 3} a^3 \rangle + 4\gamma_p \langle a^\dagger a \rangle \\ \frac{d\langle a^{\dagger 2} a^3 \rangle}{dt} = (-i\omega_c - 2iU + 5\chi - 4\kappa) \langle a^{\dagger 2} a^3 \rangle - (iU + 5\kappa) \langle a^{\dagger 3} a^4 \rangle + 6\gamma_p \langle a^{\dagger 2} a^2 \rangle \\ \frac{d\langle a^{\dagger 3} a^2 \rangle}{dt} = (i\omega_c + 2iU + 5\chi - 4\kappa) \langle a^{\dagger 3} a^2 \rangle - (-iU + 5\kappa) \langle a^{\dagger 4} a^3 \rangle + 6\gamma_p \langle a^{\dagger 2} a \rangle \\ \frac{d\langle a^{\dagger 3} a^3 \rangle}{dt} = (6\chi - 6\kappa) \langle a^{\dagger 3} a^3 \rangle - 6\kappa \langle a^{\dagger 4} a^4 \rangle + 9\gamma_p \langle a^{\dagger 2} a^2 \rangle \\ \frac{d\langle a^{\dagger 3} a^4 \rangle}{dt} = (-i\omega_c - 3iU + 7\chi - 9\kappa) \langle a^{\dagger 3} a^4 \rangle + 12\gamma_p \langle a^{\dagger 2} a^3 \rangle \\ \frac{d\langle a^{\dagger 4} a^3 \rangle}{dt} = (i\omega_c + 3iU + 7\chi - 9\kappa) \langle a^{\dagger 4} a^3 \rangle + 12\gamma_p \langle a^{\dagger 3} a^2 \rangle \\ \frac{d\langle a^{\dagger 4} a^4 \rangle}{dt} = (8\chi - 12\kappa) \langle a^{\dagger 4} a^4 \rangle + 16\gamma_p \langle a^{\dagger 3} a^3 \rangle \end{array} \right. \quad (S9)$$

Solving Eqs. (S8) and (S9), we can obtain $G^R(\omega) = \langle\langle a; a^\dagger \rangle\rangle_\omega$. The characteristic frequencies ω_0 of the single-particle excitation spectra are the poles of $G^R(\omega)$, i.e., $[G^R(\omega_0)]^{-1} = 0$. In Fig. (3) of the main text, we show the real and imaginary parts of the characteristic frequencies ω_0 . We find that the single-particle excitation spectra are divided into four branches. When the imaginary parts of ω_0 are negative, the noise state is stable, otherwise the steady state is unstable and a new coherent state emerges. In this coherent state, all non-diagonal terms of Eq. (S4) are nonzero. And the mean-field theory is more suitable to describe this case; see the following section. We emphasize that in the noise state, the photons are localized in each cavity, which is crucial for many-body steady-state phase transition, as shown in the main text.

B. MEAN-FIELD STEADY-STATE PHASE TRANSITION OF SINGLE CAVITY

In this section, we present a mean-field steady-state phase transition of the incoherent-pumped dissipative single cavity. To do this, we first turn Eq. (S1) into the frequency space, i.e.,

$$\omega \langle\langle a; a^\dagger \rangle\rangle_\omega = 1 + (\omega_c + i\chi) \langle\langle a; a^\dagger \rangle\rangle_\omega + (U - i\kappa) \langle\langle a^{\dagger 2} a^2; a^\dagger \rangle\rangle_\omega, \quad (S10)$$

where $\langle\langle a; a^\dagger \rangle\rangle_\omega$ is the retard Green's function in the frequency space and its inverse determines the single-particle excitation spectra [3]. This equation is not a closed equation of $\langle\langle a; a^\dagger \rangle\rangle_\omega$, since it is decided by the second-order time-ordered correlation function $\langle\langle a^{\dagger 2} a^2; a^\dagger \rangle\rangle_\omega$. Obviously, we cannot directly derive the required single-particle excitation spectra of single cavity from Eq. (S10), unless we take some approximation.

In the spirit of the mean-field approximation, the photon distribution in the cavity can be described by a classical photon field, characterized by a pair of complex variables. Thus, we split the operators a and a^\dagger into their steady-state expectation values and quantum fluctuations, i.e.,

$$a = \alpha + \delta\alpha, \quad a^\dagger = \alpha^* + \delta\alpha^\dagger, \quad (S11)$$

where $\alpha = \langle a \rangle$ and $\alpha^* = \langle a^\dagger \rangle$ are the mean-field amplitudes, and $\delta\alpha$ and $\delta\alpha^\dagger$ are the fluctuation operators. The complex variables α and α^* fully specify the coherent properties of steady state and the mean-photon number can be defined as $n = |\alpha|^2$. Meanwhile, the stability of steady state is decided by the dynamics of $\delta\alpha$ and $\delta\alpha^\dagger$ [1]. If only considering the quadratic term of fluctuations in $\langle\langle a^\dagger a^2; a^\dagger \rangle\rangle_\omega$, we simplify Eq. (S10) as a closed equation,

$$\omega \langle\langle \delta\alpha; \delta\alpha^\dagger \rangle\rangle_\omega = 1 + (\omega_c + i\chi) \langle\langle \delta\alpha; \delta\alpha^\dagger \rangle\rangle_\omega + (U - i\kappa) |\alpha|^2 \langle\langle \delta\alpha; \delta\alpha^\dagger \rangle\rangle_\omega, \quad (\text{S12})$$

where $|\alpha|^2$ should be determined self-consistently. We assume that at the initial time the system is in the vacuum state, with $|\alpha|^2 = 0$, and then the pumping is switched on adiabatically. In this case, the non-zero mean-field amplitudes appear when the pumping strength crosses a critical value. This critical point can be calculated by the dispersion relation of the vacuum state, which is encoded in the poles of the inverse of the retard Green's function, i.e.,

$$\omega = \omega_c + i\chi. \quad (\text{S13})$$

For $\chi < 0$, the single-particle excitation decays in time and the vacuum state is stable, whereas for $\chi > 0$, the vacuum state becomes instable and the fully dispersion relation is given by

$$\omega = \omega_c + U |\alpha|^2 + i(\chi - \kappa |\alpha|^2), \quad (\text{S14})$$

which has a steady solution, with $|\alpha|^2 = \chi/\kappa$. Based on the above analysis, we find a mean-field steady-state phase transition of the incoherent-pumped dissipative single cavity, from a incoherent vacuum state, with $\langle a \rangle = 0$ and $\langle a^\dagger a \rangle = 0$, to a coherent classical state, with $\langle a \rangle \neq 0$ and $\langle a^\dagger a \rangle \neq 0$, at the critical point $\chi_c = 0$. This phase transition is independent of the photon-photon interaction. This mean-field approximation can well describe the physical phenomena in the deep coherent-state region. However, it cannot capture the behavior in the critical region. The main reason is that this method has neglected the important environment-induced quantum-fluctuation effect, governed by the higher-order time-ordered correlation functions in the incoherent state; see the main text for details.

C. MEAN-FIELD MANY-BODY STEADY-STATE PHASE TRANSITION

In this section, we present a mean-field many-body steady-state phase transition of the 2D incoherent-pumped dissipative Bose-Hubbard model.

When replaced a_i by $\alpha_i = \langle a_i \rangle$ in the 2D Bose-Hubbard Hamiltonian (2) of the main text and assumed that all sites are identical, i.e., $\alpha_i = \alpha_j$, the initial many-body problem is reduced to a single-site problem, which is governed by the following equation:

$$\frac{d\alpha}{dt} = \left[-i \left(\omega_c - J + U |\alpha|^2 \right) + \chi - \kappa |\alpha|^2 \right] \alpha. \quad (\text{S15})$$

We can obtain self-consistent solutions of Eq. (S15) by assuming $\alpha = \alpha_0 \exp[-i(\omega_c - J + \mu)t]$, where $\mu = U |\alpha_0|^2$ is introduced as an effective chemical potential for dynamical stability [4]. The mean-photon number $|\alpha|^2$ is derived from the real part on the right-hand of Eq. (S15). For example, for $\chi < 0$, Eq. (S15) only have a zero solution, with $\langle a \rangle = \langle a^\dagger \rangle^* = \alpha_0 = 0$. This means that the photon field have no coherent part and the system is in an incoherent

vacuum state, with $\langle a^\dagger a \rangle = |\alpha|^2 = 0$. For $\chi > 0$, there exists a stationary solution, with $|\alpha_0|^2 = \chi/\kappa$. In this case, the system is in a coherent classical state, with $\langle a \rangle = \langle a^\dagger \rangle^* = a_0 \exp(-i\mu t)/\sqrt{2}$ and $\langle a^\dagger a \rangle = |a_{cl}|^2/2 = \chi/\kappa$. In conclusion, based on Eq. (S15), a mean-field many-body steady-state phase transition of the 2D incoherent-pumped dissipative Bose-Hubbard model, from the incoherent vacuum state to the coherent classical state, is predicted at the critical point $\chi_c = 0$.

D. MANY-BODY STEADY-STATE PHASE TRANSITION USING THE CONTINUOUS-FIELD APPROXIMATION

In this section, we present a many-body steady-state phase transition of the 2D incoherent-pumped dissipative Bose-Hubbard model, using the continuous-field approximation in the Keldysh functional-integral formalism

We first write a Keldysh partition function, which is fully equivalent to the many-body Lindblad master equation (1) of the main text, as [3]

$$Z = \int \mathcal{D}[a_+, a_-] \exp[iS_K(a_+, a_-)], \quad (\text{S16})$$

where $+$ and $-$ denote the forward and backward branches, and S_K is the Keldysh action. By introducing the coherent (H) and dissipative (D) terms, the Keldysh action is given by

$$S_K = S_H + S_D, \quad (\text{S17})$$

where

$$S_H = \sum_i \int_t \left\{ \left[a_{i+}^\dagger (i\partial_t - \omega_c) a_{i+} - \frac{U}{2} a_{i+}^\dagger a_{i+}^\dagger a_{i+} a_{i+} \right] - \left[a_{i-}^\dagger (i\partial_t - \omega_c) a_{i-} - \frac{U}{2} a_{i-}^\dagger a_{i-}^\dagger a_{i-} a_{i-} \right] \right\} \\ + \frac{J}{z} \sum_{\langle i,j \rangle} \int_t \left[a_{i+}^\dagger a_{j+} - a_{i-}^\dagger a_{j-} \right], \quad (\text{S18})$$

$$S_D = -i\gamma_p \sum_i \int_t \left[a_{i+}^\dagger a_{i-} - \frac{1}{2} (a_{i+} a_{i+}^\dagger + a_{i-} a_{i-}^\dagger) \right] - i\gamma_l \sum_i \int_t \left[a_{i+} a_{i-}^\dagger - \frac{1}{2} (a_{i+}^\dagger a_{i+} + a_{i-}^\dagger a_{i-}) \right] \\ - i\kappa \sum_i \int_t \left\{ (a_{i+} a_{i-}^\dagger)^2 - \frac{1}{2} \left[(a_{i+}^\dagger a_{i+})^2 + (a_{i-}^\dagger a_{i-})^2 \right] \right\}, \quad (\text{S19})$$

with $\int_t = \int dt$.

For a field-theory treatment of lattice models, we can use the continuous approximation to study the long-distance behavior [5]. If $\langle a \rangle$ and $\langle a^\dagger \rangle$ are assumed to be small near the critical point, we expand the lattice operators to second-order derivative in the spatial coordinate, i.e.,

$$a_i \mapsto a_x, \quad a_{i+1} \mapsto a_x + \nabla a_x + \frac{1}{2} \nabla^2 a_x + \dots, \quad (\text{S20})$$

where we have made the lattice constant as 1. As a result, the hopping terms become

$$- \frac{J}{z} \sum_{\langle i,j \rangle} (a_i^\dagger a_j + a_j^\dagger a_i) \mapsto - \int_{\mathbf{r}} \left(J a_{\mathbf{r}}^* a_{\mathbf{r}} + \frac{J}{z} a_{\mathbf{r}}^* \nabla^2 a_{\mathbf{r}} \right), \quad (\text{S21})$$

with $\int_{\mathbf{r}} = \int dx dy$, and the coherent and dissipative Keldysh actions turn into

$$S_H = \int_{t,\mathbf{r}} \left\{ \left[a_{\mathbf{r}+}^* \left(i\partial_t - \omega_c + J + \frac{J}{z} \nabla^2 \right) a_{\mathbf{r}+} - \frac{U}{2} a_{\mathbf{r}+}^* a_{\mathbf{r}+}^* a_{\mathbf{r}+} a_{\mathbf{r}+} \right] - \left[a_{\mathbf{r}-}^* \left(i\partial_t - \omega_c + J + \frac{J}{z} \nabla^2 \right) a_{\mathbf{r}-} - \frac{U}{2} a_{\mathbf{r}-}^* a_{\mathbf{r}-}^* a_{\mathbf{r}-} a_{\mathbf{r}-} \right] \right\}, \quad (\text{S22})$$

$$S_D = -i\gamma_p \int_{t,\mathbf{r}} \left[a_{\mathbf{r}+}^* a_{\mathbf{r}-} - \frac{1}{2} (a_{\mathbf{r}+} a_{\mathbf{r}+}^* + a_{\mathbf{r}-} a_{\mathbf{r}-}^*) \right] - i\gamma_l \int_{t,\mathbf{r}} \left[a_{\mathbf{r}+} a_{\mathbf{r}-}^* - \frac{1}{2} (a_{\mathbf{r}+}^* a_{\mathbf{r}+} + a_{\mathbf{r}-}^* a_{\mathbf{r}-}) \right] - i\kappa \int_{t,\mathbf{r}} \left\{ (a_{\mathbf{r}+} a_{\mathbf{r}-}^*)^2 - \frac{1}{2} [(a_{\mathbf{r}+}^* a_{\mathbf{r}+})^2 + (a_{\mathbf{r}-}^* a_{\mathbf{r}-})^2] \right\}. \quad (\text{S23})$$

It is more convenient to discuss Eqs. (S22) and (S23) in the Keldysh basis,

$$a_{cl} = \frac{a_+ + a_-}{\sqrt{2}}, \quad a_q = \frac{a_+ - a_-}{\sqrt{2}}, \quad (\text{S24})$$

where a_{cl} and a_q are the classical and quantum fields [3], and we ignore the index \mathbf{r} for simplicity. After a straightforward calculation, the Keldysh action in the spatial coordinate is rewritten as

$$S_K = \int_{t,\mathbf{r}} \begin{pmatrix} a_{cl}^* & a_q^* \end{pmatrix} \begin{pmatrix} 0 & P^A \\ P^R & i(\gamma_p + \gamma_l) \end{pmatrix} \begin{pmatrix} a_{cl} \\ a_q \end{pmatrix} - \frac{1}{2} [(U + i\kappa) (a_{cl}^{*2} a_{cl} a_q + a_q^{*2} a_{cl} a_q) + \text{c.c.}] + 2i\kappa a_{cl}^* a_{cl} a_q^* a_q, \quad (\text{S25})$$

where c.c. denotes the complex conjugate, and the inverse retarded and advanced single-particle Green's functions are given by

$$P^R = P^{A\dagger} = i\partial_t - \omega_c + \frac{J}{2} \nabla^2 + J - i\chi. \quad (\text{S26})$$

Eq. (S25) is similar to that of Refs. [6, 7].

For the small quantum fluctuations, we employ the saddle-point approximation,

$$\frac{\delta S_K}{\delta a_{cl}^*} = 0 \quad (\text{S27})$$

and

$$\frac{\delta S_K}{\delta a_q^*} = 0, \quad (\text{S28})$$

to find the stable points. Firstly, Eqs. (S27) and (S28) lead to two equations

$$P^A a_q - \frac{1}{2} (U + i\kappa) |a_c|^2 a_q - \frac{1}{2} (U - i\kappa) (|a_q|^2 a_q + a_c^2 a_q^*) + 2i\kappa |a_q|^2 a_c = 0, \quad (\text{S29})$$

$$P^R a_c + i(\gamma_p + \gamma_l) a_q - \frac{1}{2} (U + i\kappa) |a_q|^2 a_c - \frac{1}{2} (U - i\kappa) (|a_c|^2 a_c + a_q^2 a_c^*) + 2i\kappa |a_c|^2 a_q = 0. \quad (\text{S30})$$

In terms of Eq. (S29), we obtain a solution [3]

$$a_q = 0. \quad (\text{S31})$$

Substituting Eq. (S31) into Eq. (S30) yields a steady-state equation

$$i \frac{\partial a_{cl}}{\partial t} = \left(\omega_c - J - \frac{J}{2} \nabla^2 + \frac{U}{2} |a_{cl}|^2 \right) a_{cl} + i \left(\chi - \frac{\kappa}{2} |a_{cl}|^2 \right) a_{cl}. \quad (\text{S32})$$

Based on the imaginary part on the right-hand of Eq. (S32), we can obtain self-consistent solutions. For example, for $\chi < 0$, Eq. (S32) only has a zero solution, with $a_{cl} = 0$, and the mean value of photon field is thus given by $\langle a \rangle = \langle a^\dagger \rangle^* = a_{cl}/\sqrt{2} = 0$. This implies that the photon field has no coherent part, and the system is in an incoherent vacuum state, with $\langle a^\dagger a \rangle = |a_{cl}|^2/2 = 0$. For $\chi > 0$, there exists a stationary solution, with $a_{cl} = a_0 \exp(-i\mu t)$, where $a_0 = |a_{cl}|$ and the parameter $\mu = U|a_{cl}|^2/2$ is also introduced as an effective chemical potential for dynamical stability [4]. In this case, the system is in a coherent classical state, with $\langle a \rangle = \langle a^\dagger \rangle^* = a_0 \exp(-i\mu t)/\sqrt{2}$ and $\langle a^\dagger a \rangle = |a_{cl}|^2/2 = \chi/\kappa$. The above results indicate that the positive effective gain of single photon can pump a coherent photon field and is balanced by the two-photon loss. Moreover, they demonstrate that a many-body steady-state phase transition of the 2D incoherent-pumped dissipative Bose-Hubbard model, from the incoherent vacuum state to the coherent classical state, occurs at the critical point $\chi_c = 0$.

However, the above results, similar to the mean-field predictions in Sec. (C), seem confusing, because they violate our intuitive experiences about the strong correlation problems, where we expect the photon-photon interaction in the same cavity and the photon hopping between adjacent cavities play dominate roles in the critical behavior. A possible reason is that we have assumed the environment-induced quantum fluctuations are small to ensure the validity of the saddle-point approximation in Eqs. (S27) and (S28). This approximation can be met only if the system enters the deep coherent-state region, where the pumping is strong and the coherent part of photons is large [3]. It is not surprising that the above method cannot make correct prediction about the critical behavior. To overcome this shortcoming, the environment-induced quantum fluctuations must be taken into account and a more effective method should be established, which is the main purpose of this Letter. The detailed discussions are shown in the main text as well as the following section.

E. THE NON-EQUILIBRIUM DYSON EQUATION USING NON-EQUILIBRIUM STRONG-COUPLING EXPANSION APPROXIMATION

To correctly capture the strong-correlated steady-state phase transition of the 2D incoherent-pumped dissipative Bose-Hubbard model, here we develop a non-equilibrium strong-coupling approximation in the Keldysh formalism. In this section, we mainly obtain a non-equilibrium Dyson equation.

We assume that at the initial time every cavity is in the noise state, which means that the photons are localized at each site. When increasing the hopping strength, the photons can transition between adjacent cavities. Therefore, we can present a strong-coupling expansion [8], in which all the single-site terms are regarded as the unperturbed parts and the hopping terms are treated as perturbations.

In the Keldysh basis, the many-body partition function is written as

$$Z = \int \mathcal{D}[a_{cl}, a_q] \exp[iS_0(a_{cl}, a_q) + iS_J(a_{cl}, a_q)], \quad (\text{S33})$$

where a_{cl} and a_q are the classical and quantum fields as mentioned above. The unperturbed Keldysh action in

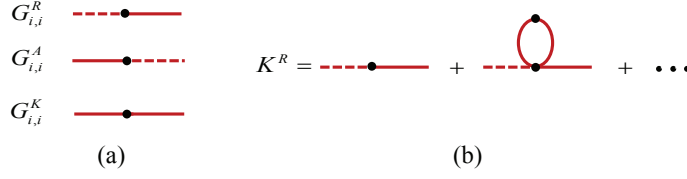


FIG. S1: (Color online) (a) Graphic representation of the on-site retard Green's function $G_{i,i}^R$, the advanced Green's function $G_{i,i}^A$, and the Keldysh Green's function $G_{i,i}^K$. The solid and dashed lines represent the classical and quantum fields a_{cl} and a_q , respectively. (b) The irreducible part of the retard Green's function K^R .

Eq. (S33) is given by

$$S_0 = \sum_i \int_t (a_{i,cl}^* a_{i,q}^*) \begin{pmatrix} 0 & [G_{i,i}^{-1}(t)]^A \\ [G_{i,i}^{-1}(t)]^R & [G_{i,i}^{-1}(t)]^K \end{pmatrix} \begin{pmatrix} a_{i,cl} \\ a_{i,q} \end{pmatrix}, \quad (\text{S34})$$

where $[G_{i,i}^{-1}(t)]^R$, $[G_{i,i}^{-1}(t)]^A$, and $[G_{i,i}^{-1}(t)]^K$ are the inverses of the on-site retard Green's function [equal to $G_0^R(t)$], advanced Green's function $G_{i,i}^A(t) = i\theta(-t)\langle[a_i(t), a_i^\dagger(0)]\rangle$, and Keldysh Green's function $G_{i,i}^K(t) = -i\langle[a_i(t), a_i^\dagger(0)]_+\rangle$, respectively. The advanced Green's function $G_{i,i}^A(t)$ can be derived straightforwardly from the relation $[G_{i,i}^A(t)] = [G_{i,i}^R(t)]^\dagger$, whereas the Keldysh Green's function $G_{i,i}^K(t)$ can be, in principle, obtained by using the similar steps as calculating $G_{i,i}^R(t)$. Similar to $G_{i,i}^R(t)$, the explicit expression of $G_{i,i}^K(t)$ is very complicate. However, here we do not present $G_{i,i}^A(t)$ and $G_{i,i}^K(t)$ explicitly, since they does not affect the main results under the first-order approximation of the photon hopping that we apply below.

Since the above three unperturbed Green's functions arise from the many-body Lindblad master equation (1) in the main text, they have a compact form

$$G_{i,i}^{\alpha\beta}(t) = \begin{pmatrix} G_{i,i}^K(t) & G_{i,i}^R(t) \\ G_{i,i}^A(t) & 0 \end{pmatrix} = -i \langle a_{i,\alpha}(t) a_{i,\beta}^*(0) \rangle_{S_0}, \quad (\text{S35})$$

where $\alpha, \beta = (cl, q)$ and the average $\langle \cdots \rangle_{S_0}$ is taken with respect to the unperturbed Keldysh action S_0 [3]. Based on Eq. (S35), we present a graphic representation of the three unperturbed Green's functions; see Fig. S1(a). The perturbation part of the Keldysh action (S33) is given by

$$S_J = \sum_{\langle i,j \rangle} \int_t \frac{J_{ij}}{z} [a_{i,cl}^* a_{j,q} + a_{i,q}^* a_{j,cl} + \text{c.c.}]. \quad (\text{S36})$$

To explore the many-body steady-state phase diagram, we should calculate the full retard Green's function

$$\tilde{G}^R(t) = -i \langle a_{i,cl}(t) a_{i,q}^*(0) \rangle_{S_0 + S_J}, \quad (\text{S37})$$

which is dressed by the hopping terms in the perturbed Keldysh action S_J . Since the unperturbed Keldysh action S_0 contains all on-site terms, it is not a normal quadratic form on the field operators. Thus, the Wick's theorem and the powerful perturbation technique, based on the standard Feynman diagrams, cannot be applied. Instead, here we use

a non-equilibrium linked-cluster expansion approach in the Keldysh basis, which gives a description of equilibrium or non-equilibrium strong correlation systems within the same formalism [3]. It has already been used to study the Bose-Hubbard model with finite temperature [9] or time-varying hopping [10]. Following this method, we sum an infinite set of diagrams by calculating the irreducible part of the retard Green's function $K^R(t)$, which is connected, in the frequency space, to the full retard Green's function via the following equation:

$$\tilde{G}^R(\mathbf{k}, \omega) = \frac{K^R(\mathbf{k}, \omega)}{1 - J(\mathbf{k}) K^R(\mathbf{k}, \omega)}, \quad (\text{S38})$$

with the 2D lattice dispersion $J(\mathbf{k}) = 2J \cos(\mathbf{k} \cdot \mathbf{r})$, where \mathbf{k} is the wave vector and \mathbf{r} denotes the lattice vector, with $|\mathbf{r}| = 1$. In Fig. S1(b), we show a chain diagram and a most relevant one-loop diagram of the retard Green's function $K^R(\mathbf{k}, \omega)$. The chain diagram denotes the first-order approximation of the photon hopping and the one-loop diagram represents the leading spatial related correction. Numerical simulations have verified that this first-order approximation can well describe the many-body steady-state properties of the 2D non-equilibrium lattice systems [11], since in such systems the higher-order corrections contain higher-order time correlation functions, which decay very fast due to the coupling with environment [9, 10]. Thus, below we will mainly consider the chain diagram of the retard Green's function $K^R(\mathbf{k}, \omega)$.

By setting $K^R(\omega) = G_{i,i}^R(\omega)$ in Eq. (S38), we immediately obtain a non-equilibrium Dyson equation about the inverse of the full retard Green's function in the momentum space, i.e.,

$$[\tilde{G}^R(\mathbf{k}, \omega)]^{-1} = [G_{i,i}^R(\omega)]^{-1} - \Sigma^R(\mathbf{k}, \omega), \quad (\text{S39})$$

where $\Sigma^R(\mathbf{k}, \omega) = J(\mathbf{k})$ is the self-energy. Based on the non-equilibrium Dyson equation (S39), we can obtain the many-body steady-state phase diagram of the 2D incoherent-pumped dissipative Bose-Hubbard model. The detailed discussions are shown in the main text.

-
- [1] D. F. Walls and G. J. Milburn, *Quantum Optics* (Springer, New York, 2008).
 - [2] In current experiments of Rydberg atoms about the multi-photon electromagnetically-induced transparency, the maximal photon number in the cavity is small and tunable. See, for example, a review, I. Carusotto and C. Ciuti, *Quantum Fluids of Light*, *Rev. Mod. Phys.* **85**, 299 (2013).
 - [3] A. Altland and B. Simons, *Condensed Matter Field Theory* (Cambridge University Press, 2010).
 - [4] J. Keeling, M. H. Szymanska, and P. B. Littlewood, in *Optical Generation and Control of Quantum Coherence in Semiconductor Nanostructures*, Nanoscience and Technology, edited by G. Slavcheva and P. Roussignol (Springer-Verlag, Berlin, 2010), pp. 293-329.
 - [5] M. F. Maghrebi and A. V. Gorshkov, Nonequilibrium many-body steady states via Keldysh formalism, *Phys. Rev. B* **93**, 014307 (2016).
 - [6] L. M. Sieberer, S. D. Hubber, E. Altman, and S. Diehl, Dynamical Critical Phenomena in Driven-Dissipative Systems, *Phys. Rev. Lett.* **110**, 195301 (2013).
 - [7] L. M. Sieberer, S. D. Hubber, E. Altman, and S. Diehl, Nonequilibrium functional renormalization for driven-dissipative Bose-Einstein condensation, *Phys. Rev. B* **89**, 134310 (2014).

- [8] W. Metzner, Linked-cluster expansion around the atomic limit of the Hubbard model, *Phys. Rev. B* **43**, 8549 (1991).
- [9] T. D. Graß, F. E. A. dos Santos, and A. Pelster, Excitation spectra of bosons in optical lattices from the Schwinger-Keldysh calculation, *Phys. Rev. A* **84**, 013613 (2011).
- [10] M. P. Kennett and D. Dalidovich, Schwinger-Keldysh approach to out-of-equilibrium dynamics of the Bose-Hubbard model with time-varying hopping, *Phys. Rev. A* **84**, 033620 (2011).
- [11] S. Finazzi, A. Le Boité, F. Storme, A. Baksic, and C. Ciuti, Corner-space renormalization method for driven-dissipative two-dimensional correlated systems, *Phys. Rev. Lett.* **115**, 080604 (2015).